Bioelectrochemistry 140 (2021) 107812

Contents lists available at ScienceDirect

Bioelectrochemistry

journal homepage: www.elsevier.com/locate/bioelechem

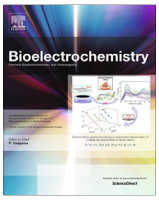

Label-free highly sensitive detection of DNA approximate length and concentration by impedimetric CRISPR-dCas9 based biosensor technology

Zihni Onur Uygun [a], Sevcan Atay [b,*]

[a] Kafkas University, Faculty of Medicine, Department of Medical Biochemistry, Kars, Turkey
[b] Ege University, Faculty of Medicine, Department of Medical Biochemistry, Bornova İzmir, Turkey

ARTICLE INFO

Article history:
Received 16 March 2021
Received in revised form 23 March 2021
Accepted 28 March 2021
Available online 31 March 2021

Keywords:
Biosensor
Chronoimpedance
Electrochemical impedance spectroscopy
Capacitance
CRISPR
dCas9

ABSTRACT

In this study, we designed a CRISPR-dCas9-based biosensor with potential clinical use in glioblastoma subtype discrimination through detection of isocitrate dehydrogenase R132H (IDH) mutation status. The electrode was modified to detect mutant DNA cysteamine (Cys), PAMAM, dCas9 and sgRNA for R132H mutations, respectively. The biosensor system we proposed was able not only to detect mutant DNA, but also to measure the approximate length of DNA. Therefore, it can be considered that the biosensor technology that we developed is novel in the field of DNA biosensors. Another superior capability of the biosensor system is that it can simultaneously measure DNA concentration by electrochemical impedance spectroscopy and DNA length by capacitive detection, which lowers the concentration-based false-positive signals. The calibration range was obtained between 100 fM and 1000 fM, LOD and LOQ were also calculated as 33.96 fM and 102.91 fM respectively. Moreover, thanks to the sensitivity of the capacitive detection, the biosensor was able to discriminate the same EIS signals of the 200 bp and 250 fM concentration data and 1000 bp and 50 fM concentration data. In conclusion, the biosensor was capable of detect target DNA and DNA length, simultaneously in minutes.

1. Introduction

Glioblastoma (GBM, WHO stage IV astrocytoma) is the most common aggressive brain tumor in adults. The average life expectancy in patients with GBM is between 11 and 19 months, who receive standard treatment including maximal surgical resection, radiotherapy, and adjuvant chemotherapy [1]. Glioblastomas are divided into two subgroups: Primary Glioblastoma and Secondary Glioblastoma. Primary glioblastomas progress rapidly without clinical or histological evidence of a less malignant precursor lesion, whereas secondary glioblastomas develop by transformation or progression of low-grade diffuse astrocytoma (WHO grade II) or anaplastic astrocytoma (WHO grade III). This transformation or progression process takes 2–5 years in secondary glioblastoma, while more than half of the primary glioblastoma cases have a clinical history of less than 3 months [2,3]. Although it is practically not possible to distinguish between primary and secondary glioblastomas from each other histologically, the genetic and epigenetic backgrounds of these two glioblastoma subtypes are quite different. One of the main molecular differences between primary and secondary glioblastomas is the presence of isocitrate dehydrogenase (IDH) mutations, which are found in approximately 75% of secondary GBM but are extremely rare in primary GBM [4]. In 2016, World Health Organization restructured the classification of glioblastomas in the light of molecular studies carried out in the field of central nervous system tumors. According to the 2016 WHO classification of tumors of the central nervous system (CNS), glioblastomas are divided into three subgroups based on isocitrate dehydrogenase 1 (IDH1) and IDH2 mutation status as IDH-wild-type (Primary GBM), IDH-mutant (Secondary GBM) and unspecified (NOS- not otherwise specified). Therefore, detection of IDH mutation status is very important for accurate diagnosis of subtypes of the disease and predicting prognosis. It has been reported that the most common IDH mutation in glioblastomas is the R132H (c.395G > A) mutation in IDH1 gene that causes an arginine/histidine amino acid change [5,6]. Detection of the IDH mutation status is carried out by DNA sequencing method, where the devices and consumables used in the analysis are quite expensive and require advanced laboratory infrastructure as well as

* Corresponding author.
E-mail address: sevcan.atay@ege.edu.tr (S. Atay).

https://doi.org/10.1016/j.bioelechem.2021.107812
1567-5394/

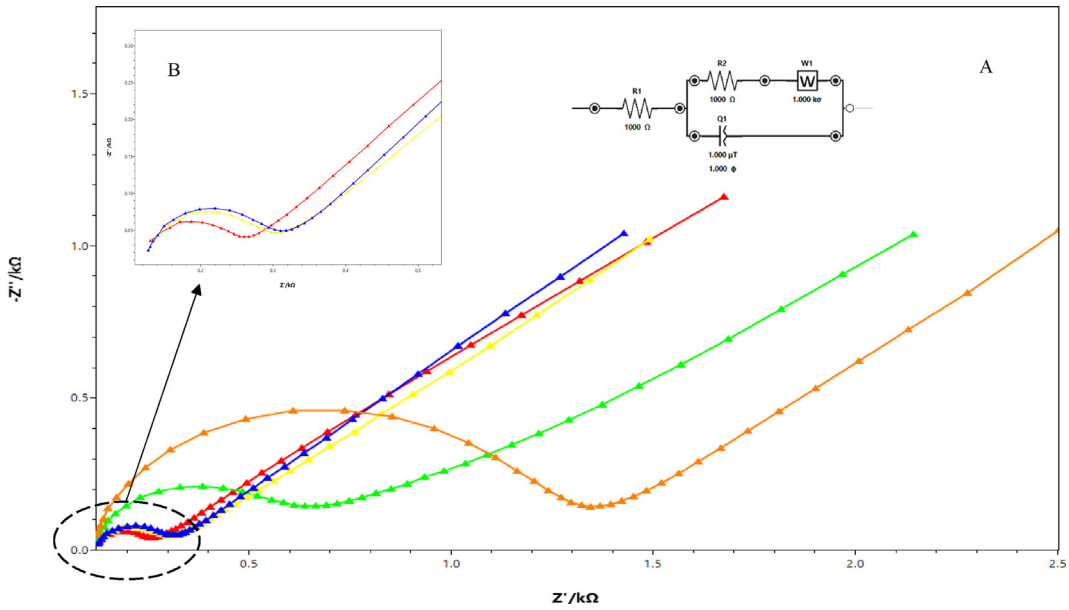

Fig. 1. EIS representation of the modification steps and circuit model (R1; redox probe solution impedance, R2; biosensor surface impedance, W1; Warburg impedance, Q1; constant phase element) of the Glioblastoma biosensor, Yellow EIS: AuE, Red EIS: AuE/Cys, Blue EIS: AuE/Cys/PAMAM, Green EIS: AuE/Cys/PAMAM/dCas9, Orange EIS: AuE/Cys/PAMAM/dCas9/sgRNA (B: Close caption of the dotted area).

well-trained and experienced personnel. In our study, a cheap, rapid, selective, and accurate CRISPR-dCas9 based electrochemical biosensor system was developed to detect the most common IDH mutation in glioblastomas.

Biosensors are miniaturized analyzers by immobilization of a biorecognition receptor such as enzyme, receptor, antibody, DNA, or protein molecule that shows affinity only to the analyte molecule, on a physicochemical transducer [7,8]. The signals resulting from the interaction between this biorecognition receptor and the analyte molecule are transduced to the analyzer system by the transducer, and the measurement is performed by analyzing the forming signal depending on the interaction between the biorecognition receptor and analyte[9,10]. Biosensors can be catalytic or affinity-based, depending on the biorecognition receptor type on the transducer [11]. As it is known, CRISPR-dCas9 system is able to use DNA molecules as biorecognition receptors for biosensor technology [12]. The dCas9 and the sgRNA are capable of binding DNA sequences specifically and sensitively, and this interaction can be used to detect DNA sequences. In biosensor systems developed for DNA detection, the effect of DNA length on electrochemical signals has not been investigated yet, and its effects on measurements are unknown. For this reason, in impedimetric measurements, it was predicted that as the DNA length increases the impedance may increase due to the increase in the negative charges. For the first time in this study, in order to minimize the charge clouding, capacitance measurement is used as a reference method besides impedance measurement.

In the presented study, while the mutant DNA sequence bound by the biorecognition receptor, deactivated Cas9, on the surface of the biosensor was measured with EIS. EIS is a powerful method that is used especially in affinity-based biosensor technology to obtain sensitive signals [13–15]. Moreover, in this study, the false-positive signals originating from DNA length were also prevented by capacitive measurement. Consequently, we developed a sensitive, practical, and rapid impedimetric/capacitive biosensor system using CRISPR-dCas9 modified with sgRNA to detect the most common IDH mutation in glioblastomas.

2. Experimental section

2.1. Materials, equipment and reagents

In this study, gold screen printed electrodes (AuE) were obtained from Dropsens 250AT (Oviedo (Asturias) Spain). dCas9 (40 µg (250 pmol/ 25 µL)) proteins were obtained from Applied Biological Materials Inc. (abm) (Richmond, BC, V6V 2 J5, Canada). sgRNA sequence (99%) (*N: target nucleotide*; 5′NNNNNNNNNNNNNNNNNNNNNNGUUUUAGAGCUAGAAAUAGCAAGUUAAAAUAAGGCUAGUCCGUUAUCAACUUGAAAAAGUGGCACCGAGUCGGUGCUUUU-3′) were synthesized by Synthego (Redwood City, CA 94063, USA). Atomic force microscopy (AFM) was carried out by using BRUKER Dimension Edge with ScanAsyst (Bruker USA). Other consumables and chemicals as HPLC grade were obtained from Merck (Darmstadt, Germany). Redox probe solution was prepared as mentioned in previous reports [12].We used Palmsens 3 Potentiostat/Galvanostat/EIS analyzer and PSTrace 5.8 as interface. EIS curves were calculated by using the circuit model as shown in Fig. 1.

2.2. Biosensor modification

Electrochemical analysis of the electrode surfaces was carried out by performing CV and EIS in redox probe [12]. CV was performed by applying potential between −0.2 to 0.5 V with a scan rate of 100 mV/s. EIS was performed between the frequency of 10,000 to 0.05 Hz by applying 180 mV DC and 10 mV AC. Prior to use, AuE was washed with triple distilled water and soaked in ethanol solution, which contains 100 mM cysteamine (Cys), to self-assembly monolayer (SAM) formation for one hour. Afterwards, AuE was washed with absolute ethanol and pure water,

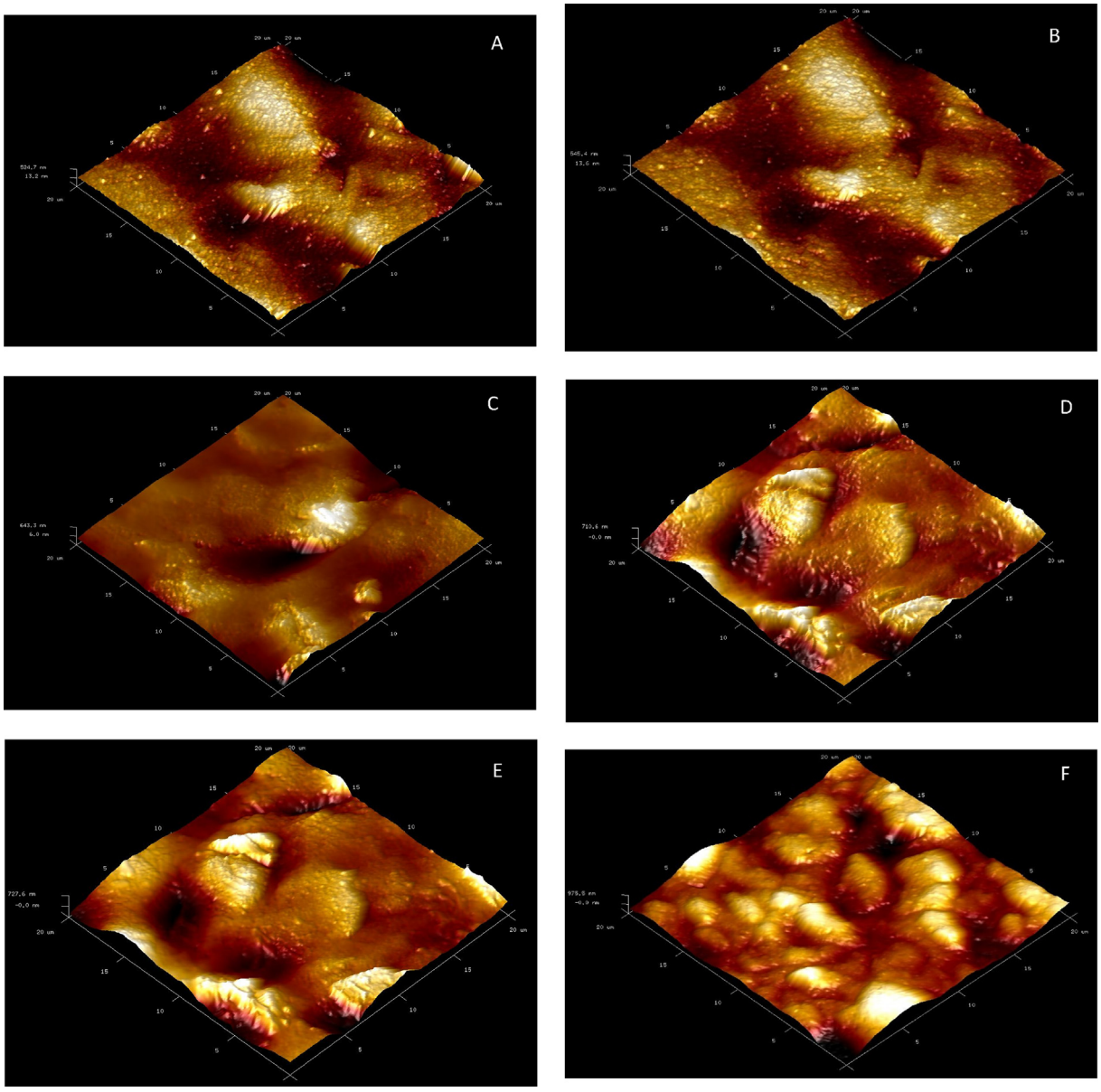

Fig. 2. Biosensor modification steps with atomic force microscope (AFM) (A: AuE, B: AuE/Cys, C: AuE/Cys/PAMAM, D: AuE/Cys/PAMAM/dCas9, E: AuE/Cys/PAMAM/dCas9/sgRNA, F: AuE/Cys/PAMAM/dCas9/sgRNA/DNA).

respectively. AuE/Cys modified electrode then activated by dropping 50 μL 5% (v/v) glutaraldehyde solution for 30 min. Subsequently, 20 μL of amine functionalized poliamidoamin (PAMAM) was dropped on electrode. AuE/Cys/PAMAM electrode was activated once more with glutaraldehyde for dCas9 modification. dCas9 proteins were immobilized on the PAMAM modified electrodes via glutaraldehyde links for one night in moisturized environment at + 4^{O}C and unbounded dCas9 proteins were washed by ultrapure water. In order to prevent misbinding of the sgRNA, unbounded active by glutaraldehyde PAMAM and Cys residues were blocked by glisin amino acid. Then, AuE/Cys/PAMAM/dCas9 electrode was modified by sgRNA sequence to target the IDH mutation. When the biosensor was successfully constructed, optimization studies were performed calibration curve, LOD, LOQ, effect of DNA length, reproducibility and repeatability.

3. Results and discussion

3.1. Biosensor modifications

Although our biorecognition receptor was a mutant enzyme, it is an affinity-based biosensor. AuE modification layers were observed by EIS (Fig. 1A and B) and AFM (Fig. 2A to E). In those figures, CV and EIS work to form a complementary data to confirm each EIS and CV. AuE data was obtained as baseline. AuE/Cys modification was observed increase of the conductivity and decrease of the impedance because positively charged cysteamine groups attracts negatively charged redox probe [16], therefore Warburg impedance becomes dominant as mass transfer resistance. PAMAM modification of the electrode works as Cys modification because of the positively charged amino groups,

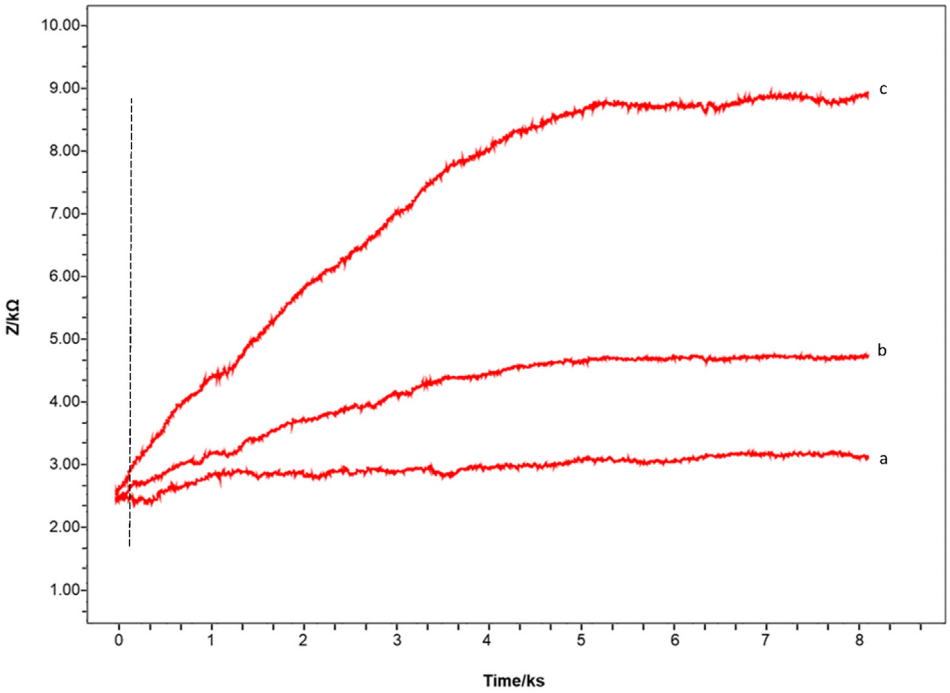

Fig. 3. Chronoimpedimetric detection of the 200 bp gliobastoma DNAs a: baseline, b: wild type, c: mutant DNA.

but it shows in Fig. 1 ethylene cores increases impedance. Afterwards, dCas9 protein, sgRNA and DNA standard immobilization also increase the impedance and decrease the peak current of the CV data.

In Fig. 2, all modifications are shown as topographic AFM images. As it can be seen that modification layers increase the surface thickness. The images approve the impedimetric results of the immobilization. DNA binding and increasing negative charges increases the surface smoothness.

3.2. Glioblastoma biosensor optimization

In the optimization steps, the biosensor was firstly tested chronoimpedimetrically. Chronoimpedance has an advantage to obtain exact analyte detection time and optimization of the target molecule the detection time [17]. The chronoimpedimetric detection is based on the Bode plot of the impedimetric detection of the prepared biosensor. The frequency is chosen, when the impedance shows increasing character and phase angle is constant, applied potential should be low to prevent that a highly polar molecule DNA is repelled from the surface [18,19]. Therefore, we applied 100 mV DC, 10 mV AC potentials and 100 Hz frequency, which is chosen from the Bode Plot of the AuE/Cys/PAMAM/dCas9/sgRNA impedance data (Fig. 1A-orange). The chronoimpedimetric detection was shown in Fig. 3. In Fig. 3, DNA detection time was shown. As it can be seen in Fig. 3a, there is a base line of the biosensor that performed in buffer without DNA, 3b shows wild type (non-mutant) DNA signal and 3c is the target mutant DNA. When the biosensor shows a saturation signal around 5kSec, wild type (non-target) molecule shows a signal even if the signal is low. Therefore, for a strong recognition of the target molecule, we used chronoimpedance to obtain detection time chronoimpedance to prevent false positive signals. As a result, chronoimpedimetric data showed that 100 s is optimized for 200 bp DNA detections.

In order to prepare a calibration plot to detect DNA concentration, impedimetric signals as Ohm were used (Fig. 4A) on y-axis and DNA concentrations as fM were used on x-axis (Fig. 4B). The concentration of DNA was detected between 100 and 1000 fM and regression coefficient was calculated for eight calibration curves as R^2 = 0.988 ± 0.004. The low DNA concentration was achieved by the increase of the surface area by PAMAM dendrimers. Reproducibility was also tested by preparing the biosensor eight times and SD was found as 0.004, which means repeatability of the biosensor was also good by comparing regression coefficient and linearity is really promising for the calibration range. 100 fM was tested 5times and found as 1781 ± 47.75 CV% was 2.68. Afterwards, LOD and LOQ were also calculated [16] as 33.96 fM and 102.91 fM, respectively.

Detection of DNA in fluids are a challenging factor because DNA length is a problem for the affinity-based biosensors. The concentration and the signal can be misinterpreted. Therefore, we investigated the DNA length effect on impedance signals and obtained promising results for further DNA based biosensor studies. Fig. 5A and B show the effect of DNA length on impedance signals. 5A blue EIS represents the 200 bp and 250 fM concentration data and red EIS represents 1000 bp and 50 fM concentration data. As it can be seen in Fig. 5A even the different concentrations are captured by the surface with close EIS their capacitive double layer differs. The main reason that the increase of the negatively charged phosphate groups decreases the double layer capacitive current (Fig. 4B). However, different concentration increases the EIS and decreases the capacitance. This method, which stands for the use of EIS and Capacitance for DNA biosensors, can be used to detect a variety of distinctive biomarkers. On the other hand, it should be considered that capacitive detection may be affected by DNA base composition and charges of the DNA molecules.

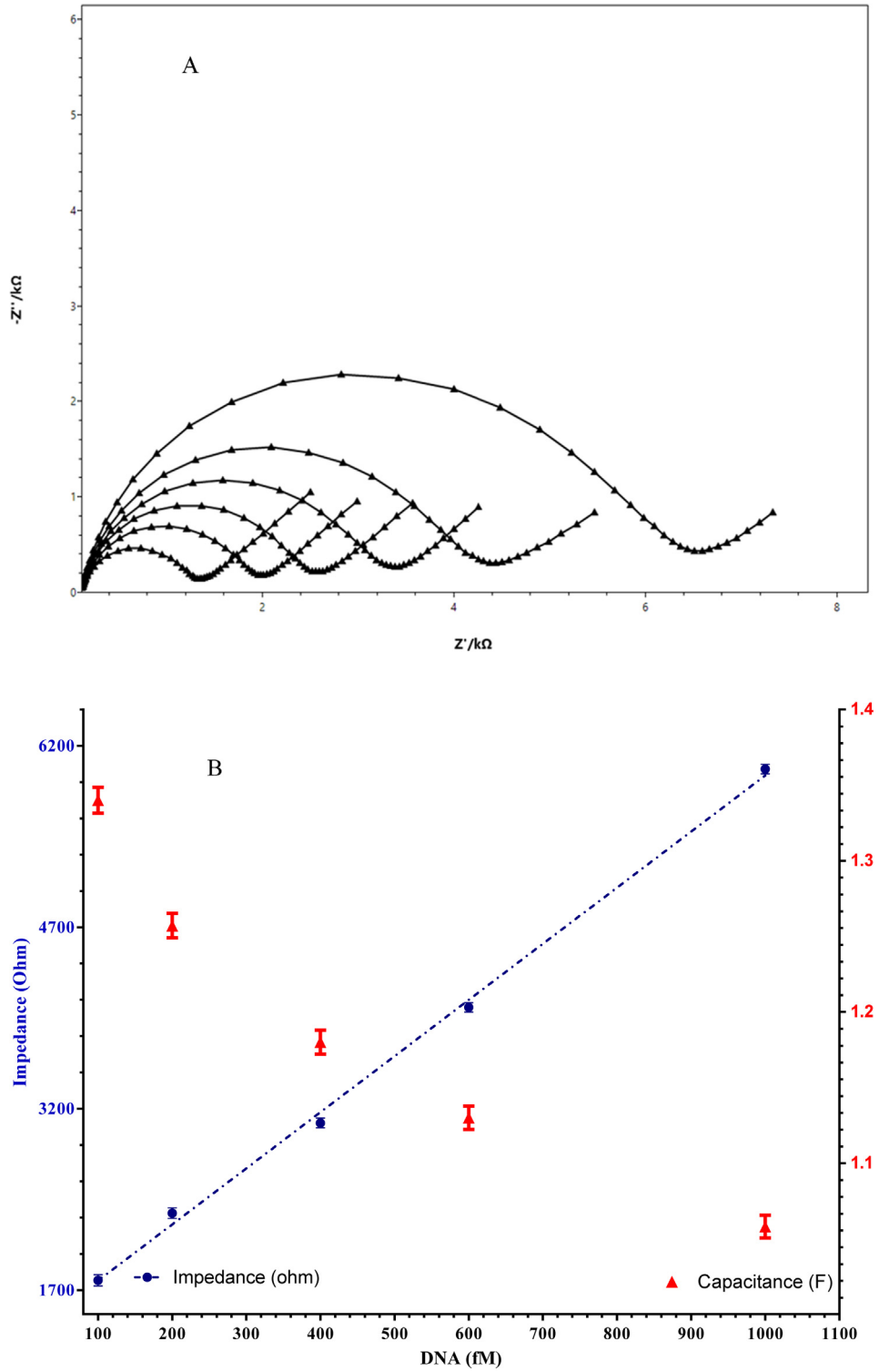

Fig. 4. . A and B. Calibration curves of Glioblastoma biosensor shown by EIS (100–1000 fM), B: calibration curve was plotted against y-axis impedance (RSD ~ 2.64 for EIS and ~ 0,67 for C) versus x-axis 200 bp DNA concentration (fM) (y = 4.640x + 1314, R^2 = 0.988).

4. Conclusion

In conclusion, we developed a biosensor technology to detect the most common IDH mutation in glioblastomas. A screen-printed gold electrode modified with a surface area increasing method to reach fM levels and chronoimpedimetric detection was used to measure detection time. The biosensor showed good linearity between 100 and 1000 fM. Moreover, for the first time in literature, we used capacitive signals for the DNA length detections. All in all, a very selective and specific CRISPR-dCas9 based biosensor system was developed and successfully reported.

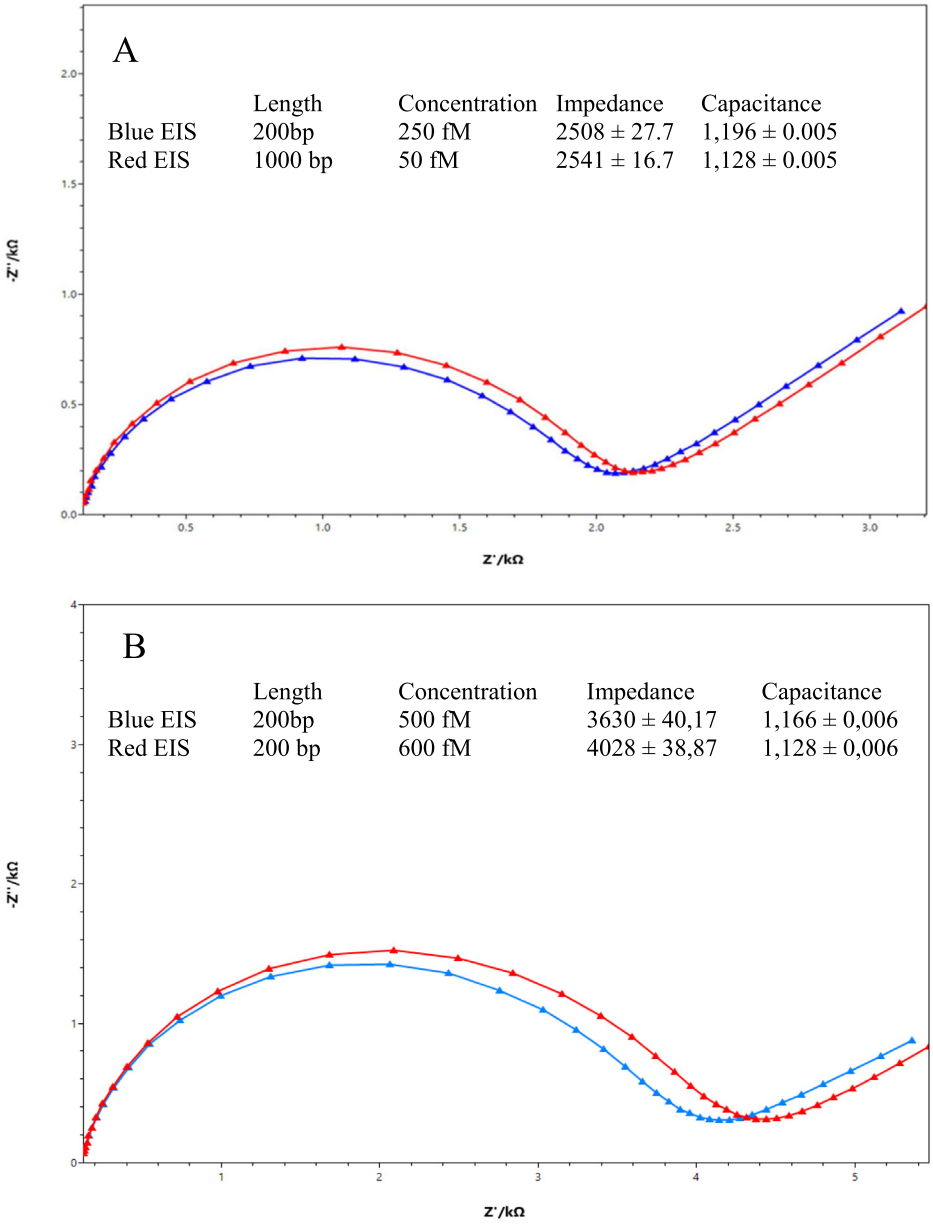

Fig. 5. . A and B. Target DNA detection with dCas9 biosensor, A: Different concentration and different length of the target DNA, B: same length and different concentration of the target.

Declaration of Competing Interest

The authors declare that they have no known competing financial interests or personal relationships that could have appeared to influence the work reported in this paper.

Acknowledgements

Authors are thankful by support of Ege University Scientific Research Projects Coordination (TGA-2020-22230).

References

[1] S.A. Grossman, X. Ye, S. Piantadosi, S. Desideri, L.B. Nabors, M. Rosenfeld, J. Fisher, Survival of patients with newly diagnosed glioblastoma treated with radiation and temozolomide in research studies in the United States, Clin. Cancer Res. 16 (2010) 2443–2449, https://doi.org/10.1158/1078-0432.CCR-09-3106.

[2] H. Ohgaki, P. Dessen, B. Jourde, S. Horstmann, T. Nishikawa, P.L. Di Patre, C. Burkhard, D. Schüler, N.M. Probst-Hensch, P.C. Maiorka, N. Baeza, P. Pisani, Y. Yonekawa, M.G. Yasargil, U.M. Lütolf, P. Kleihues, Genetic pathways to glioblastoma: A population-based study, Cancer Res. 64 (2004) 6892–6899, https://doi.org/10.1158/0008-5472.CAN-04-1337.

[3] H. Ohgaki, P. Kleihues, Population-based studies on incidence, survival rates, and genetic alterations in astrocytic and oligodendroglial gliomas, J. Neuropathol. Exp. Neurol. 64 (2005) 479–489, https://doi.org/10.1093/jnen/64.6.479.

[4] N.K. Kloosterhof, L.B.C. Bralten, H.J. Dubbink, P.J. French, M.J. van den Bent, Isocitrate dehydrogenase-1 mutations: A fundamentally new understanding of diffuse glioma?, Lancet Oncol. 12 (2011) 83–91, https://doi.org/10.1016/S1470-2045(10)70053-X.

[5] A.L. Cohen, S.L. Holmen, H. Colman, IDH1 and IDH2 mutations in gliomas, Curr. Neurol. Neurosci. Rep. 13 (2013) 345, https://doi.org/10.1007/s11910-013-0345-4.

[6] C. Hartmann, J. Meyer, J. Balss, D. Capper, W. Mueller, A. Christians, J. Felsberg, M. Wolter, C. Mawrin, W. Wick, M. Weller, C. Herold-Mende, A. Unterberg, J.W. M. Jeuken, P. Wesseling, G. Reifenberger, A. von Deimling, Type and frequency of IDH1 and IDH2 mutations are related to astrocytic and oligodendroglial differentiation and age: A study of 1,010 diffuse gliomas, Acta Neuropathol. 118 (2009) 469–474, https://doi.org/10.1007/s00401-009-0561-9.

[7] H. Karimi-Maleh, M. Alizadeh, Y. Orooji, F. Karimi, M. Baghayeri, J. Rouhi, S. Tajik, H. Beitollahi, S. Agarwal, V.K. Gupta, S. Rajendran, S. Rostamnia, L. Fu, F. Saberi-Movahed, S. Malekmohammadi, Guanine-Based DNA Biosensor Amplified with Pt/SWCNTs Nanocomposite as Analytical Tool for Nanomolar Determination of Daunorubicin as an Anticancer Drug: A Docking/Experimental Investigation, Ind. Eng. Chem. Res. 60 (2021) 816–823, https://doi.org/10.1021/acs.iecr.0c04698.
[8] H. Karimi-Maleh, F. Karimi, M. Alizadeh, A.L. Sanati, Electrochemical Sensors, a Bright Future in the Fabrication of Portable Kits in Analytical Systems, Chem. Rec. 20 (2020) 682–692, https://doi.org/10.1002/tcr.201900092.
[9] A. Khodadadi, E. Faghih-Mirzaei, H. Karimi-Maleh, A. Abbaspourrad, S. Agarwal, V.K. Gupta, A new epirubicin biosensor based on amplifying DNA interactions with polypyrrole and nitrogen-doped reduced graphene: Experimental and docking theoretical investigations, Sensors Actuators, B Chem. 284 (2019) 568–574, https://doi.org/10.1016/j.snb.2018.12.164.
[10] M. Alizadeh, P.A. Azar, S.A. Mozaffari, H. Karimi-Maleh, A.-M. Tamaddon, A DNA Based Biosensor Amplified With ZIF-8/Ionic Liquid Composite for Determination of Mitoxantrone Anticancer Drug: An Experimental/Docking Investigation, Front. Chem. 8 (2020) 814, https://doi.org/10.3389/fchem.2020.00814.
[11] N.J. Ronkainen, H.B. Halsall, W.R. Heineman, Electrochemical biosensors, Chem. Soc. Rev. 39 (2010) 1747, https://doi.org/10.1039/b714449k.
[12] Z.O. Uygun, L. Yeniay, G. Sağın, Ferhan, CRISPR-dCas9 powered impedimetric biosensor for label-free detection of circulating tumor DNAs, Anal. Chim. Acta 1121 (2020) 35–41, https://doi.org/10.1016/j.aca.2020.04.009.
[13] D. Harmanci, Z. Onur Uygun, A. Koçak Sezgin, C. Demirdöver, F. Girgin Sagin, G. Akdoğan, Rapid Fibroblast Cell Culture Characterization with Impedimetric Label-free Heat Shock Protein – 47 Biosensor, Electroanalysis 32 (2020) 2310–2315, https://doi.org/10.1002/elan.202060264.
[14] Z. Onur Uygun, H.D. Ertuğrul Uygun, A Novel Chronoimpedimetric Glucose Sensor in Real Blood Samples Modified by Glucose-imprinted Pyrrole-Aminophenylboronic Acid Modified Screen Printed Electrode, Electroanalysis 32 (2020) 226–229, https://doi.org/10.1002/elan.201900537.
[15] P. Miao, B. Wang, K. Han, Y. Tang, Electrochemical impedance spectroscopy study of proteolysis using unmodified gold nanoparticles, Electrochem. Commun. 47 (2014) 21–24, https://doi.org/10.1016/j.elecom.2014.07.013.
[16] Z.O. Uygun, Y. Dilgin, A novel impedimetric sensor based on molecularly imprinted polypyrrole modified pencil graphite electrode for trace level determination of chlorpyrifos, Sensors Actuators B Chem. 188 (2013) 78–84, https://doi.org/10.1016/j.snb.2013.06.075.
[17] H.D. Ertuğrul Uygun, Z.O. Uygun, E. Canbay, F. Gïrgïn Sağın, E. Sezer, Non-invasive cortisol detection in saliva by using molecularly cortisol imprinted fullerene-acrylamide modified screen printed electrodes, Talanta. 206 (2020) 120225. doi:10.1016/j.talanta.2019.120225.
[18] S. Li, H. Cui, Q. Yuan, J. Wu, A. Wadhwa, S. Eda, H. Jiang, AC electrokinetics-enhanced capacitive immunosensor for point-of-care serodiagnosis of infectious diseases, Biosens. Bioelectron. 51 (2014) 437–443, https://doi.org/10.1016/j.bios.2013.08.016.
[19] R. Vaidyanathan, S. Dey, L.G. Carrascosa, M.J.A. Shiddiky, M. Trau, Alternating current electrohydrodynamics in microsystems: Pushing biomolecules and cells around on surfaces, Biomicrofluidics. 9 (2015), https://doi.org/10.1063/1.4936300.